Tungsten Fiber Reinforced Copper Matrix Composites

A Review

David L. McDanels

O.K

19960611 140

DTIC QUALITY INSPECTED 3

NASA

S

PLASTEC 053534

Tungsten Fiber Reinforced Copper Matrix Composites

A Review

David L. McDanels
Lewis Research Center
Cleveland, Ohio

Summary

Tungsten fiber reinforced copper matrix (W/Cu) composites have served as an ideal model system with which to analyze the properties of metal matrix composites. A series of research programs were conducted to investigate the stress-strain behavior of W/Cu composites; the effect of fiber content on the strength, modulus, and conductivity of W/Cu composites; and the effect of alloying elements on the behavior of tungsten wire and of W/Cu composites. Later programs investigated the stress-rupture, creep, and impact behavior of these composites at elevated temperatures. Analysis of the results of these programs has allowed prediction of the effects of fiber properties, matrix properties, and fiber content on the properties of W/Cu composites. These analyses formed the basis for the rule-of-mixtures prediction of composite properties which has been universally adopted as the criteria for measuring composite efficiency. In addition, the analyses allowed extrapolation of potential properties of other metal matrix composites and were used to select candidate fibers and matrices for development of tungsten fiber reinforced superalloy composite materials for high-temperature aircraft and rocket engine turbine applications. This report summarizes the W/Cu composite efforts conducted at NASA Lewis Research Center, describes some of the results obtained, and provides an update on more recent work using W/Cu composites as high-strength, high-thermal-conductivity composite materials for high heat flux, elevated-temperature applications.

Introduction

Fiber-reinforced metal matrix composites offer a wide range of material properties for potential materials to meet specific design and application requirements. They combine the strength and modulus of a fiber with the ductility and oxidation resistance of a matrix (fig. 1). Most of the current emphasis on metal matrix composites is on low-density, high-modulus fibers, such as graphite, silicon carbide, or boron, to reinforce matrices of aluminum, magnesium, titanium, or intermetallics. Most of the applications being considered for metal matrix composites are in a relatively low temperature range. Spacecraft applications include antenna and structural applications where the temperatures range from 366 K (200 °F) in the sun to 166 K (−200 °F) in shadow conditions. Airframe applications range up to 478 K (400 °F) for supersonic flight regimes. For applications such as these, the high room-temperature strength/density and stiffness/density of composites offer major design advantages.

However, the propulsion system environment in aircraft or spacecraft presents a much more severe set of operating conditions. Increased engine efficiency and reduced fuel burn are the prime goals sought by engine designers. These goals place significant challenges on engine materials since these goals can only be gained through the use of lower weight materials, higher creep-strength/density materials, higher temperature operation, and increased rotational speed with its accompanying increased stress on rotating components (ref. 1).

The main emphasis of metal matrix composite research at NASA Lewis Research Center has traditionally been focused on materials for aircraft engine applications. The majority of these applied research programs have been aimed at two main areas of engine components: creep-resistant tungsten fiber reinforced superalloy matrix composites for the high-temperature turbine section of the engine (ref. 2); and bird-strike-resistant boron fiber reinforced aluminum matrix composites for the fan section (ref. 3).

NASA Lewis efforts on metal matrix composites have traditionally been focused on the improvement of high-temperature properties. The first step in the development of composites for elevated-temperature service was to fabricate and analyze a metal matrix composite model system. This model system was used to analyze the behavior of the model composite and to generate a data base to allow prediction of properties for other composite systems. The tungsten fiber reinforced copper matrix (W/Cu) composite system was chosen as a model to analyze the behavior of metal matrix composites. These results were used by NASA Lewis Research Center to publish the first systematic, indepth analysis of the behavior of metal matrix composites in 1959 (ref. 4) and the first mass-reader publication on metal matrix composites in 1960 (ref. 5).

Tungsten fiber reinforced copper matrix composites served as an ideal model system to analyze the behavior of metal matrix composites because the two components—tungsten wire and copper matrix—were mutually insoluble in each other, were readily available at low cost, and were easily fabricated into composites by liquid infiltration. The availability of materials allowed fabrication of large numbers of test specimens
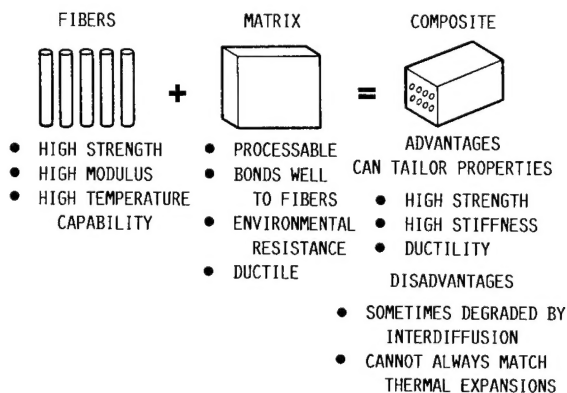
Figure 1.— Advantages and disadvantages of combining a fiber and a matrix into a composite.

covering a range of fiber contents and fiber diameters. The mutual insolubility of the components allowed a detailed analysis of the stress-strain behavior to determine the contributions of each component to the properties of the composite.

A series of research programs were conducted to investigate the stress-strain behavior of W/Cu composites; the effect of fiber content on the strength, modulus, and electrical conductivity of W/Cu composites; and the effect of alloying elements on the behavior of tungsten wire and of W/Cu composites. Later programs investigated the stress-rupture, creep, and impact behavior of these composites at elevated temperatures. These results were used to select candidate fibers and matrices for the development of usable tungsten fiber reinforced superalloy composite materials for high-temperature aircraft and rocket engine turbine applications. This report summarizes the W/Cu composite efforts conducted at NASA Lewis Research Center, describes some of the results obtained, and provides an update on more recent work using W/Cu composites as high-strength, high-thermal-conductivity composite materials for high heat flux, elevated-temperature applications.

Materials and Fabrication

The basic W/Cu model composite work used commercially drawn type 218CS-tungsten filament wire (General Electric Co.). This wire was selected for study because of its high tensile strength, its high recrystallization temperature, its availability in a wide range of diameters, and its relative ease of handling.

Oxygen-free, high-conductivity (OFHC) copper was selected as the primary matrix material for these composites. This choice was based on copper's melting point (below a temperature where the properties of the tungsten wire are seriously degraded by recrystallization), its insolubility in tungsten, and the ability of molten copper to wet tungsten. In addition,

copper alloys also were used as matrix materials. Selected alloying additions were added to the pure copper matrix to determine their effect on the behavior of the tungsten wire and on the properties of the composites.

Composites were fabricated by liquid phase infiltration. Continuous undirectional tungsten fibers were packed in ceramic tubes to the desired fiber content. A slug of copper was placed above the fiber bundle, and the assembly was placed in a furnace and heated to 1478 K (2200 °F) for 1 hr in either a vacuum or hydrogen atmosphere. The molten copper flowed over the tungsten fibers by gravity and capillarity and fully infiltrated the fiber bundle to form a sound, fully dense composite. After infiltration, the composite rods were removed from the ceramic tubes. Some rods were centerless ground into test specimens, while others had threaded grips brazed onto their ends to make threaded, round test specimens.

This method of fabrication allowed production of large numbers of fully dense, pore-free composites, with accurately aligned unidirectional fiber orientation, to be used for analysis of the behavior of W/Cu composites. All testing was done in the longitudinal direction, and all properties were determined in the direction parallel to the fiber axis.

Stress-Strain Behavior of Tungsten Fiber Reinforced Copper Matrix Composites

Analysis of the stress-strain curve of metal matrix composites is the key to understanding the behavior and predicting the mechanical properties of composites. The W/Cu composite system is an ideal model to evaluate the stress-strain behavior of composites (refs. 6 and 7). Tungsten and copper are mutually insoluble and have no interfacial reaction. Both the fiber and the matrix undergo plastic deformation at failure, and the properties of each component are very reproducible and consistent.

A set of stress-strain curves of W/Cu composites is presented in figure 2. These curves show that there are four stages of deformation in a ductile-fiber/ductile-matrix composite, such as W/Cu. These stages are shown schematically in figure 3 for the fiber, matrix, and composite. The stress on the composite, at any point on the stress-strain curve, can be represented by a volume-percent-weighted rule-of-mixtures relation connecting the stress on the fiber and the stress on the matrix at the strain at that point on the curve:

$$\sigma_c^* = \sigma_f^* V_f + \sigma_m^* V_m \qquad (1)$$

where σ is the stress, V is the volume fraction, and the subscripts c, f, and m refer to the composite, fiber, and matrix respectively. The superscript * refers to the stress on each
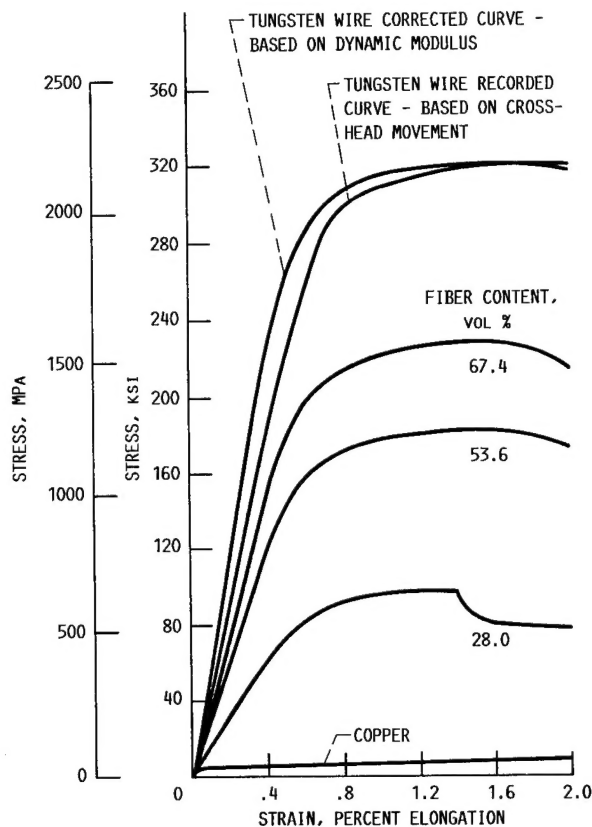
Figure 2.—Stress-strain curves for tungsten wire, copper, and tungsten fiber reinforced copper matrix composites (refs. 6 and 7).

gives rise to a secondary modulus E'' which can be predicted by

$$E_c'' = E_f V_f + \left(\frac{d\sigma_m}{d\epsilon} V_m \right) \qquad (3)$$

where $(d\sigma_m/d_\epsilon)$ is the slope of the stress-strain curve of the plastically deforming matrix. A plot of the secondary modulus of elasticity of W/Cu composites, measured from stress-strain curves, is presented in figure 5 over a range of fiber contents. The line shown on the curve represents a least-squares fit of the data, and the endpoints fall at the near-zero slope of the
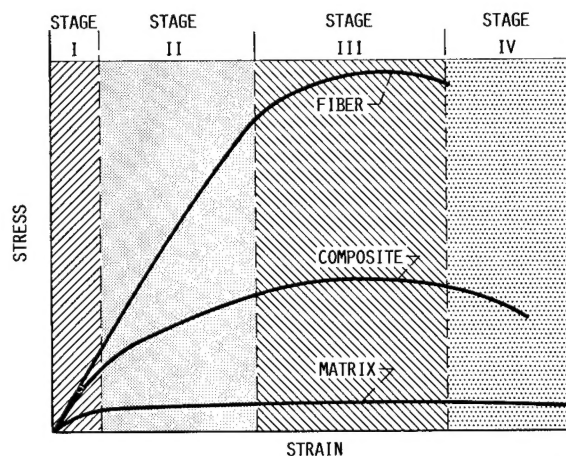

Figure 3.—Schematic representation of four stages of stress-strain behavior of metal matrix composites (after refs. 6 and 7).

component at the same strain and in the condition in which it exists within the composite.

In stage I behavior, both the fiber and the matrix undergo elastic strain. Since each component is straining elastically, the composite also exhibits elastic behavior. The modulus of elasticity of the composite E_c can be predicted by using a rule-of-mixtures relation connecting the moduli of the fiber and the matrix:

$$E_c = E_f V_f + E_m V_m \qquad (2)$$

This linear relation between the moduli of the fiber and the matrix is shown by a plot of the dynamic modulus of elasticity data from W/Cu composites over a range of fiber contents (fig. 4). The line shown on the figure represents the rule-of-mixtures prediction connecting the modulus of the copper matrix with that of the tungsten fiber.

In stage II behavior, the fibers continue to strain elastically, but the matrix has passed into plastic strain. For W/Cu composites, the fibers continue to strain elastically to about 0.4 percent strain, while the copper matrix only strains elastically to about 0.04 percent strain. This strain transition
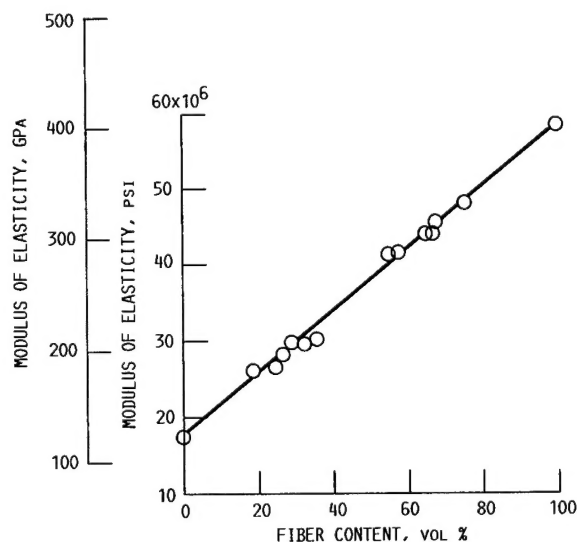

Figure 4.—Dynamic modulus of elasticity of tungsten, copper, and tungsten fiber reinforced copper matrix composites (refs. 6 and 7).
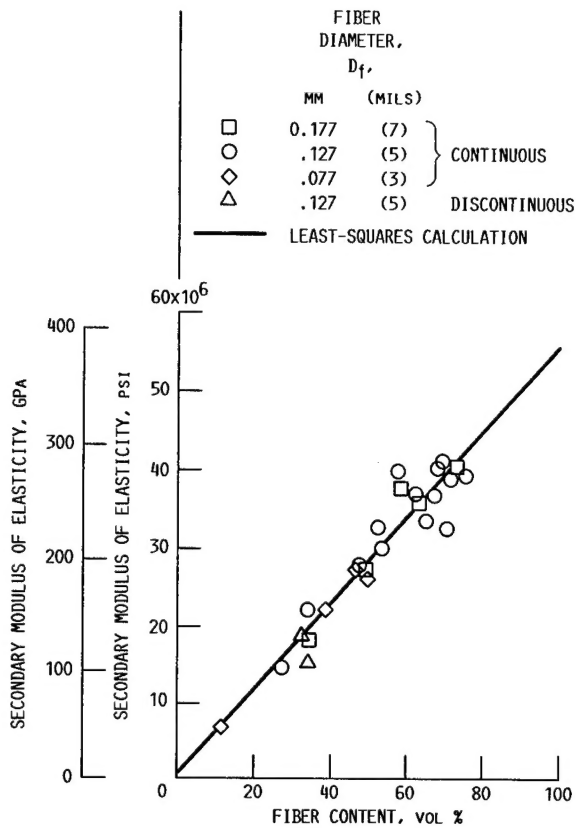
3

FIBER
DIAMETER,
D_f,

	MM	(MILS)	
□	0.177	(7)	
○	.127	(5)	CONTINUOUS
◇	.077	(3)	
△	.127	(5)	DISCONTINUOUS

——— LEAST-SQUARES CALCULATION

Figure 5.—Secondary modulus of elasticity of tungsten fiber reinforced copper matrix composites (refs. 6 and 7).

strength, based on offset from the initial modulus should not be significantly different from that based on the secondary modulus. The line shown represents a least-squares fit of the data obtained. Extrapolation of this curve to the endpoints shows good agreement with the anticipated yield strengths of the copper matrix and the tungsten reinforcing fiber.

Stage III behavior continues until the ultimate strength of the fiber is reached, which coincides with the strain where the ultimate tensile strength of the composite is also reached. The ultimate tensile strength of the W/Cu composites can be predicted using the equation:

$$\sigma_c = \sigma_f V_f + \sigma_m^* V_m \qquad (5)$$

where σ_m^* is the stress on the matrix at the strain at which the fiber reaches its ultimate tensile strength. Ultimate tensile strengths of W/Cu composites are presented in figure 7 over a range of fiber contents. The line shown on the figure represents the rule-of-mixtures prediction from equation (5). The experimental data for W/Cu composites show excellent agreement with the predicted ultimate strength line.

During stage IV behavior, the fibers reach their ultimate tensile strength and start to fail. Initially, the fibers start to break at random locations. Eventually, fiber breaks align in a failure plane and the remaining fibers in that cross section

stress-strain curve of the plastically deforming copper matrix and at the initial modulus of the still-elastic tungsten fiber.

In stage III behavior, both the fiber and matrix are straining plastically. Again, the stress on the composite is equal to a volume-percent-weighted rule-of-mixtures relation with the stress on the fiber and on the matrix at the same equivalent strain. The yield strength of the composite can be predicted by

$$\sigma_{y_c} = \sigma_{y_f} V_f + \sigma_m' V_m \qquad (4)$$

where σ_m' is the stress on the matrix at the strain at which the yield strength of the fiber is measured. For most matrices, stress increases due to work hardening are not significant over this strain range, compared with the differences in strength between the fiber and the matrix. Therefore the value of the yield strength of the matrix σ_{y_m} could be substituted for the value of σ_m' in equation 4, if actual stress-strain data are not available. Yield strength data for W/Cu composites are shown in figure 6. The yield strengths of the composites were calculated using a 0.2 percent offset, based on the secondary modulus for convenience of measurement. Because the copper stress-strain curve was flat in the plastic region, the yield
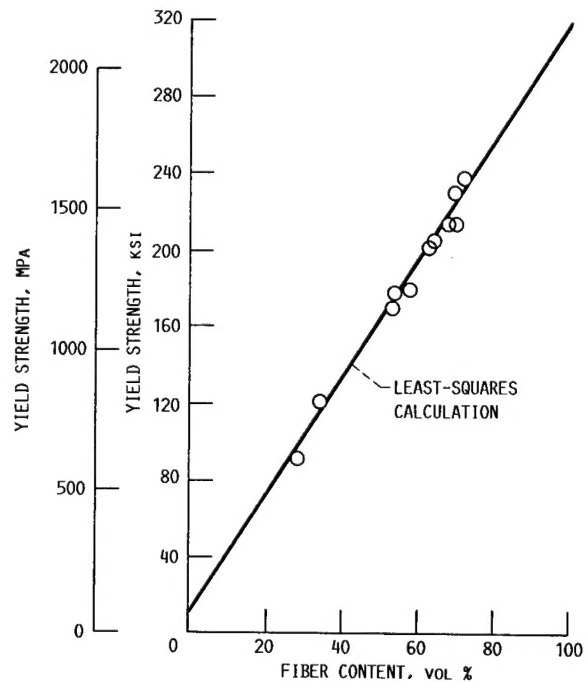

Figure 6.—Yield strength (based on secondary modulus) of tungsten fiber reinforced copper matrix composites (refs. 6 and 7).
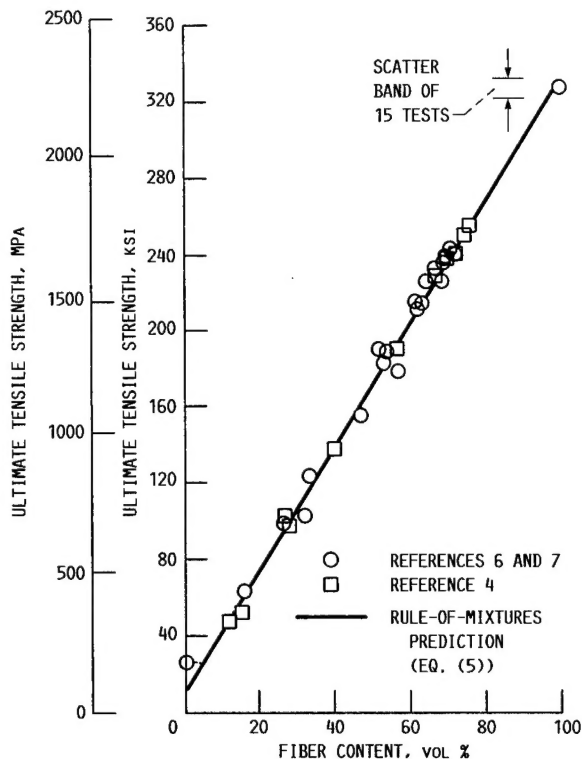
Figure 7.—Ultimate tensile strength of tungsten fiber reinforced copper matrix composites (refs. 6 and 7).

Properties of Composites Reinforced With Discontinuous Fibers

All of the composites discussed previously were reinforced with continuous unidirectional tungsten fibers. Other composites were fabricated with uniaxially oriented, discontinuous-fiber reinforcement and tested in the direction parallel to the fibers. Tungsten wire, 0.127 mm (5 mil) in diameter, was chopped to lengths of 0.975 mm (0.375 in.), and infiltrated with copper. Results of tensile tests on these composites, with a reinforcing-fiber length-to-diameter aspect ratio of 75, are shown in figure 10 for a range of fiber contents. The ultimate tensile strengths of the composites showed good agreement with the rule-of-mixtures prediction line used for composites reinforced with continuous fibers.

Although the stress-strain behavior and tensile strength relations observed for discontinuous-fiber-reinforced
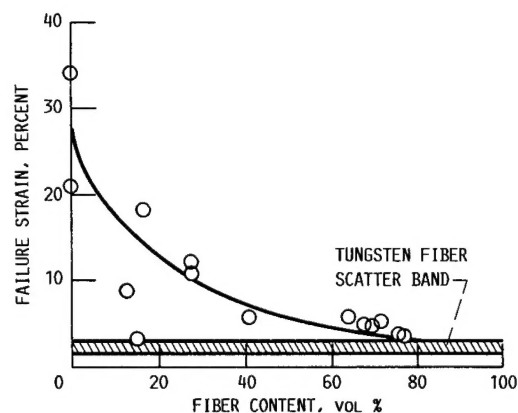

Figure 8.—Failure strain of tungsten fiber reinforced copper matrix composites (refs. 6 and 7).

fail, and the load drops rapidly. The composite is then held together by ligatures of ductile, unreinforced matrix that continue to strain until they also fail. The stress on the composite drops as these ligatures break.

The effect of fiber content on failure strain is shown over a range of fiber contents in figure 8. At low fiber content, matrix ligatures were of sufficient size to continue to strain, with the composite reaching a strain to failure of 10 percent or more and the remaining copper forming a localized point of unreinforced copper before the last ligature failed. At higher fiber contents, the composite strain to failure dropped to about 4 to 5 percent. Since the fibers broke at about 2 to 3 percent strain, the weakest fibers (with the lowest failure strains) broke first, and the composite continued to strain at nearly full load until the main fracture plane was established. After the fibers at the fracture plane had broken, additional strain on the composite occurred in the unreinforced copper ligatures only, at very low stresses.

The rule-of-mixtures relation was also observed for tensile test results for W/Cu composites at elevated temperatures. The ultimate tensile strengths of W/Cu composites are plotted as a function of fiber content in figure 9 for a series of temperatures up to 1255 K (1800 °F) (ref. 8). Results of tensile tests on pure copper were also reported for temperatures up to 1089 K (1500 °F) and on type 218CS-tungsten wire up to 922 K (1200 °F).
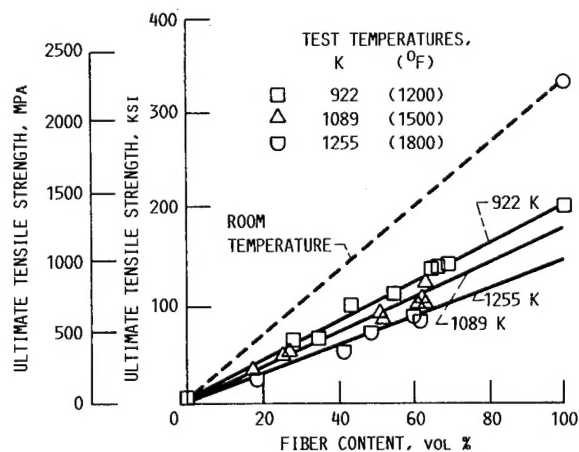

Figure 9.—Ultimate tensile strength of tungsten fiber reinforced copper matrix composites at various temperatures (data from ref. 8).
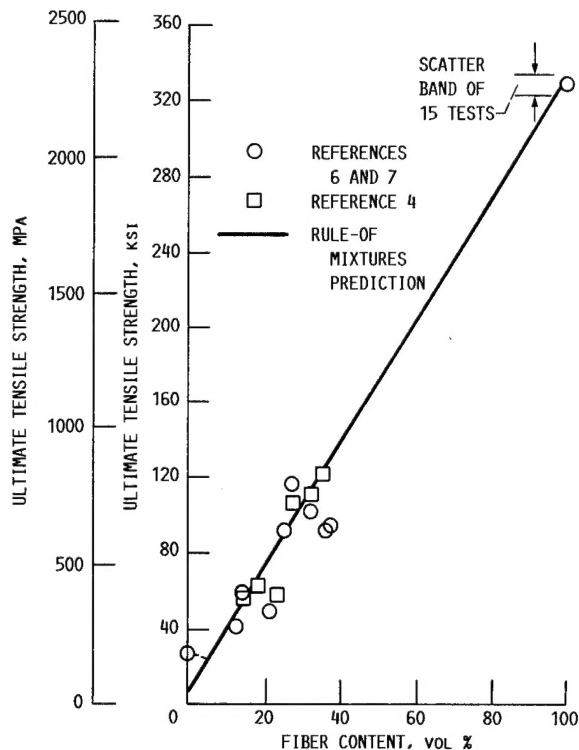
5

Figure 10.—Ultimate tensile strength of copper matrix composites reinforced with discontinuous tungsten wires; fiber aspect ratio, 75, (refs. 6 and 7).

composites are similar to those observed for composites with continuous reinforcement, the mechanism by which such composites are strengthened is different. In a composite reinforced with continuous fibers, the load is carried by the fibers along their full length. When random fiber breaks appear, part of the load is carried around this break by interfacial shear transfer through the interface and the matrix. In a composite reinforced with discontinuous fibers, however, all the load must be carried from fiber to fiber by interfacial shear transfer through the matrix.

The stress distribution along the length of a discontinuous fiber is shown schematically in figure 11 (refs. 9 and 10). The ends of the fibers, called the ineffective length, can carry a very high shear stress but can carry only a low tensile stress. Thus, short-length fibers will not contribute their full tensile strength to a composite. At longer lengths, the shear stress and tensile stress will balance and the fiber can support the full tensile load. The length at which a portion of the fiber starts to carry a stress equal to its full tensile strength is called the critical length L_{crit} and may be calculated by

$$L_{crit} = \sigma_f \frac{D_f}{2\tau} \qquad (6)$$

where σ_f is the tensile strength of the fiber, D_f is the fiber diameter, and τ is the shear strength of the matrix. At L_{crit},

the average tensile strength of the fiber will be one-half of its ultimate tensile strength. As the fiber length gets longer, a greater portion of the fiber will be able to carry its full tensile stress. For a continuous fiber, the ineffective length at the ends of the fiber becomes insignificant and the average fiber tensile strength will be equal to its ultimate tensile strength. For a discontinuous fiber, the ineffective length at the ends of the fibers cannot carry a full tensile load, and the average tensile stress that can be carried by a discontinuous fiber is the ratio of the effective length $(L - L_{crit})$ to the total fiber length L as given by

$$\sigma_{f,av} = \sigma_{f,max} \left(1 - \frac{L_{crit}}{2L} \right) \qquad (7)$$

where $\sigma_{f,av}$ is the average fiber stress, $\sigma_{f,max}$ is the ultimate tensile strength of the fiber, L is the fiber length, and L_{crit} is the critical length of the fiber. The tensile strength of a discontinuous-fiber reinforced composite depends on the tensile strength of the fiber, the length of the reinforcing fiber, and the shear strength of the matrix or of the fiber/matrix interface, whichever is lesser. This calculation of the average fiber strength for discontinuous-fiber reinforcement modifies the composite strength prediction of equation (5) to

$$\sigma_c = \sigma_f \left(1 - \frac{L_{crit}}{2L} \right) V_f + \sigma_m^* V_m \qquad (8)$$

Thus, at longer fiber lengths, the ultimate tensile strength of discontinuous-fiber composites will approach that of continuous-fiber composites. As the aspect ratio decreases, the composite strength decreases, but the composite will still fail in tension. At fiber lengths below L_{crit}, the composite will fail by shear pullout of the fiber from the matrix at a much lower stress than for the continuous-fiber composites.

The effect of fiber aspect ratio on the tensile strength of copper matrix composites reinforced with discontinuous fibers becomes more important at elevated temperatures because the shear strength of the copper matrix is reduced. The effect of several low fiber aspect ratios was reported in reference 10
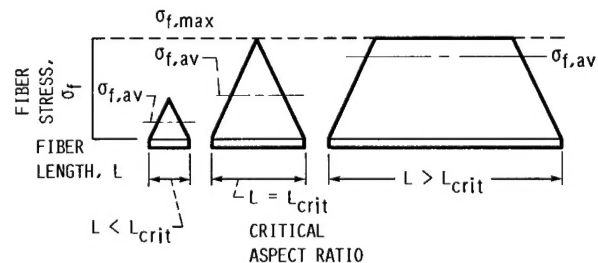

Figure 11.—Tensile stress gradients on fibers of various lengths (refs. 9 and 10).

for discontinuous-fiber reinforced W/Cu composites tested at 523 K (482 °F). The deviations from continuous-fiber composite behavior increased significantly with decreasing fiber aspect ratio (fig. 12).

Results reported in reference 9 show that W/Cu composites, reinforced with discontinous fibers of higher aspect ratios, can exhibit high strengths at elevated temperatures. Composites with a discontinous-fiber aspect ratio of 200 approached the strength values predicted for continuous-fiber reinforced composites at 755 K (900 °F), whereas composites reinforced with fibers with an aspect ratio of 100 had lower strengths. Similar trends were observed for W/Cu composites tested at 1089 K (1500 °F), except that the deviation from continuous-fiber behavior was greater (fig. 13). At fiber aspect ratios of 200, the W/Cu composites failed in tension, but at lower strengths than the continuous-fiber composites. At fiber aspect ratios of 100, the W/Cu composites appeared to be approaching the critical aspect ratio. Some composites failed in tension, while others failed by shear pullout of the fiber from the matrix at lower stresses.

A detailed study was conducted to determine the critical aspect ratio for W/Cu composites at various temperatures (ref. 11). A pullout specimen was used, in which a hole was drilled into tungsten buttons of various thicknesses. A 0.254-mm-(10-mil-) diameter tungsten fiber was placed in the hole, and copper was infiltrated between the wire and walls of the hole. Tensile tests were conducted by pulling on the bare end of the wire and on the button. The fiber shear length was determined by the thickness of the tungsten button. For longer shear lengths, failure occurred by tensile failure of the tungsten wire (fig. 14). At shorter shear lengths, the wire remained intact and pulled out of the matrix in a shear pullout failure. The critical aspect ratio was experimentally measured
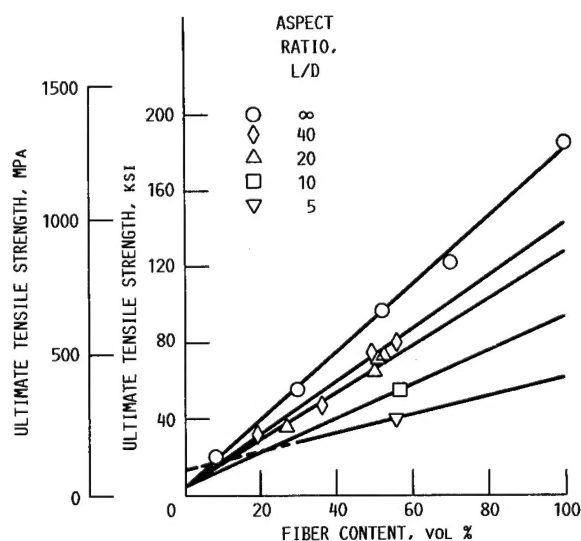

Figure 13.—Effect of aspect ratio on ultimate tensile strength of tungsten fiber reinforced copper matrix composites reinforced with discontinuous tungsten wire tested at 1089 K (1500 °F) (ref. 9).
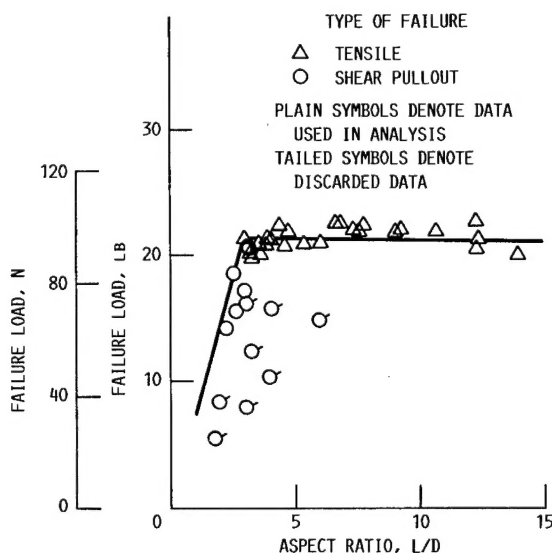
Figure 14.—Effect of aspect ratio on failure load and failure mode of tungsten-wire/copper-matrix pullout specimens (ref. 11).

by determining the aspect ratio where failure underwent a transition from shear pullout to fiber tensile failure. The experimentally determined critical aspect ratio increased with increasing temperature (fig. 15). The rise was fairly minor up to 755 K (900 °F), but increased rapidly above this temperature.

The fracture behavior of unidirectional discontinuous-fiber W/Cu composites is also influenced by the orientation of the fibers. There are three potential fracture modes in fiber-reinforced composites: tensile failure of the fiber, shear failure at the fiber/matrix interface, and tensile failure of the matrix (fig. 16). A composite will fail at the lowest strength condition predicted from these three potential failure modes at a given fiber orientation (ref. 9). At very low angles from uniaxiality,

Figure 12.—Effect of aspect ratio on ultimate tensile strength of tungsten fiber reinforced copper matrix composites reinforced with discontinuous tungsten wire tested at 523 K (482 °F) (ref. 10).
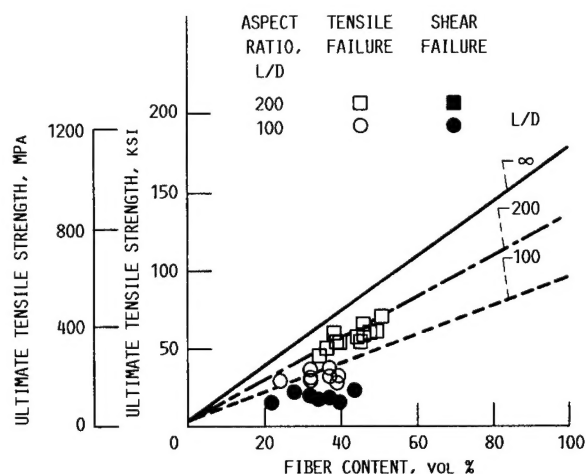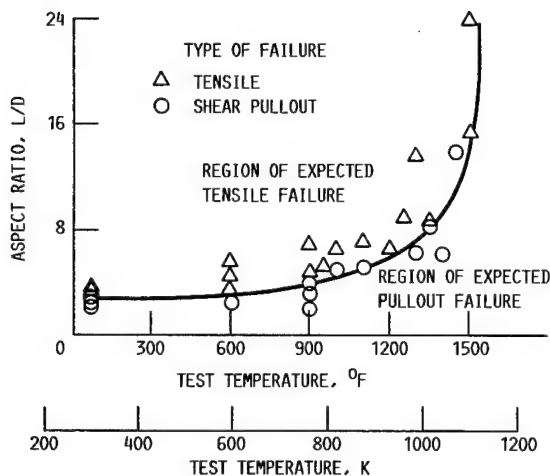
7

Figure 15.—Effect of test temperature on critical aspect ratio for tungsten-wire/copper-matrix pullout shear specimens (ref. 11).

Figure 17.—Composite strength as a function of fiber content and orientation for copper matrix composites reinforced with discontinuous tungsten fibers; fiber aspect ratio, 100 at 1089 K (1500 °F) (ref. 9).
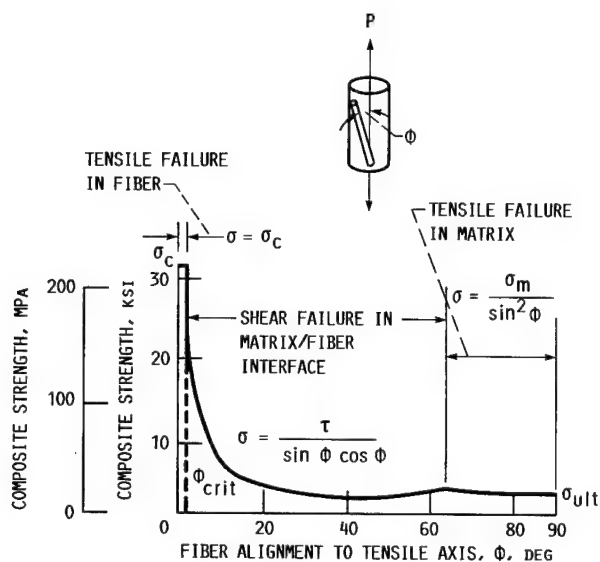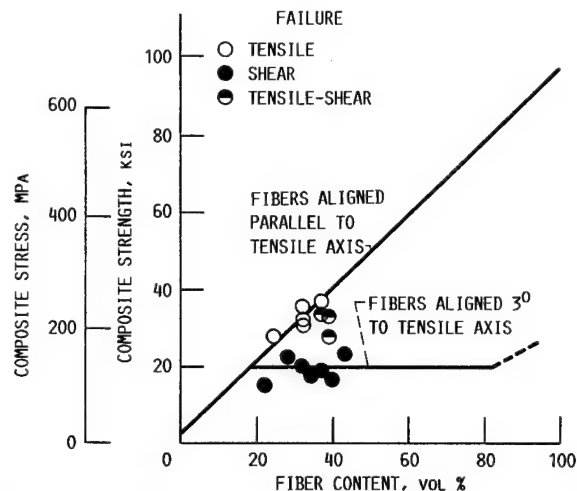

Figure 16.—Effect of fiber alignment on strength of discontinuous tungsten fiber reinforced copper matrix composites (ref. 9).

a composite will fail at a high stress by tensile failure of the fiber. With increasing misalignment, the fracture mode changes to a shear failure at the fiber/matrix interface, with an accompanying large decrease in strength. At a fiber misalignment of about 65°, the fracture mode changes to a tensile failure in the matrix.

These calculations indicate the importance of maintaining axiality in discontinuous-fiber reinforced composites. As the temperature increases, the matrix shear strength drops rapidly, thus reducing the allowable misalignment of fibers for effective composite reinforcement. At a temperature of 1089 K (1500 °F), composite strength starts to drop at a misalignment of about 0.5°. With misalignments of only 3°, shear pullout failure predominates (fig. 17), and the composite strength drops by one-half (ref. 9). Thus, for discontinuous-

fiber reinforced composites, maintenance of axiality is very important, much more so than with continuous-fiber reinforcement.

Effect of Alloying Additions on Properties of Tungsten Fiber Reinforced Copper Matrix Composites

The previously described model studies of W/Cu composites used a pure copper matrix which was insoluble in tungsten. The effect of reactive matrices on composite properties was studied by using copper binary alloy matrices containing elements with varying solubility in tungsten (refs. 12 and 13). The composites were tested at room temperature, and a microstructural analysis was made to determine the types of reactions occurring at the fiber/matrix interface. The tensile strengths of the tungsten fiber/copper-alloy matrix composites studied were reduced to some degree when alloying with the tungsten fibers occurred. Several of the composite systems studied, however, showed very little reduction in tensile strength relative to composites made with a pure copper matrix.

Three types of reactions were observed to occur at the tungsten fiber/copper-alloy matrix interface: (1) a diffusion-penetration reaction accompanied by recrystallization of the grains at the periphery of the tungsten wire, (2) formation of a two-phase zone, and (3) a solid solution reaction without subsequent recrystallization. The first type of reaction was observed with alloying additions of cobalt, aluminum, and nickel and caused significant degradation of composite strength properties. The second type of reaction was observed with alloying additions of titanium and zirconium. The third type of reaction was observed with additions of niobium and
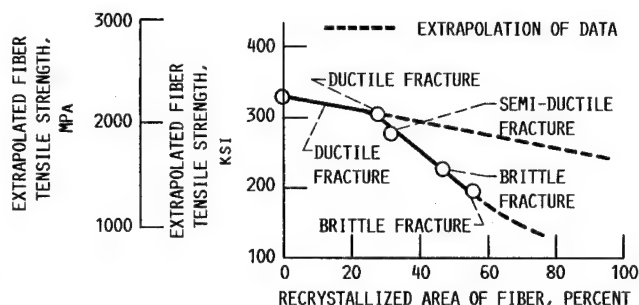
Figure 18.—Effect of recrystallized area on extrapolated tensile strength of fiber for tungsten fiber reinforced copper—5 wt % cobalt alloy matrix composites (refs. 12 and 13).

chromium. These last two types of reactions did not seriously affect the properties of the composites studied (refs. 12 and 13).

A correlation between the tensile strength and ductility of the composite was observed. In general, those materials that had the best strengths also had the best ductilities. The strength and ductility behavior was also correlated with depth of penetration measurements (refs. 12 and 13). The greater the penetration of the alloying element into the tungsten wires (causing a greater percentage of the fiber area to be recrystallized), the lower the tensile strength and ductility of the composite (fig. 18). Property degradation of the composite was greater than that predicted by the simple rule-of-mixtures relation based on the volume fractions of the reaction zone and the still-intact fiber. This fact, along with the observed correlations between the ductility and tensile strength of the fibers in the composite, suggested that damage was due to a notch-embrittling effect. It was also found that the diffusion-triggered penetration-recrystallization reaction at the fiber/matrix interface could be prevented by combining the damaging alloying element with one that did not cause this type of reaction and that was compatible with the fiber.

Stress-Rupture and Creep Properties of Tungsten Fiber Reinforced Copper Matrix Composites

The initial analyses of W/Cu composites focused on the short-time tensile properties of composites. However, in high-temperature aircraft engine applications, the long-term creep behavior and stress-rupture properties are of greater importance. A series of programs were conducted to analyze the stress-rupture properties and creep behavior of W/Cu composites by using an analysis similar to that used for stress-strain and tensile behavior predictions.

During the initial phases of this program, the stress-rupture properties of 0.127-mm-(5-mil-) diameter 218CS-tungsten wire were determined over a temperature range from 922 to 1644 K (1200 to 2500 °F). The stress-rupture tests for the wire were conducted in a specially designed testing apparatus

described in reference 14. Results of these tests (ref. 15) are shown in figure 19. Tungsten wire retained its fibrous microstructure and exhibited ductile fracture behavior at temperatures up to 1255 K (2000 °F). At a test temperature of 1533 K (2300 °F), the tungsten wire undergoes a transition in behavior. At short rupture times, the microstructure of the wire retains its heavily worked condition, while at longer times and higher temperatures, recrystallization starts to remove the strong, ductile fibrous structure and replace it with more equiaxed recrystallized grains, causing reduced strength and ductility in the fiber.

Composites were fabricated using type 218CS-tungsten wire and a pure copper matrix. Stress-rupture and creep tests were conducted at temperatures of 922 K and 1089 K (1200 and 1500 °F). A creep curve of typical W/Cu composites at each test temperature is shown in figure 20. Analysis of the creep behavior of the composite, combined with the creep behavior of the copper matrix, allowed calculation of the creep behavior of the tungsten wire, which could not be measured directly (ref. 16).

Analysis of the creep curves of a number of W/Cu specimens indicated that there are seven stages of creep behavior in a ductile-fiber/ductile-matrix metal matrix composite such as W/Cu. Schematic creep curves for the composite, fiber, and matrix are shown in figure 21(b), and the stress distribution between the fiber and the matrix is shown schematically in figure 21(a). The first stage consists of initial elastic loading, analogous to a high-temperature tensile test, where both the tungsten fibers and copper matrix carry a portion of the load proportional to their elastic modulus. The load carried by each component can be predicted by using the stage I analysis of stress-strain behavior at the stress level used in the creep test.

After a fiber/matrix stress equilibrium is reached during initial loading, the composite starts to elongate with time by
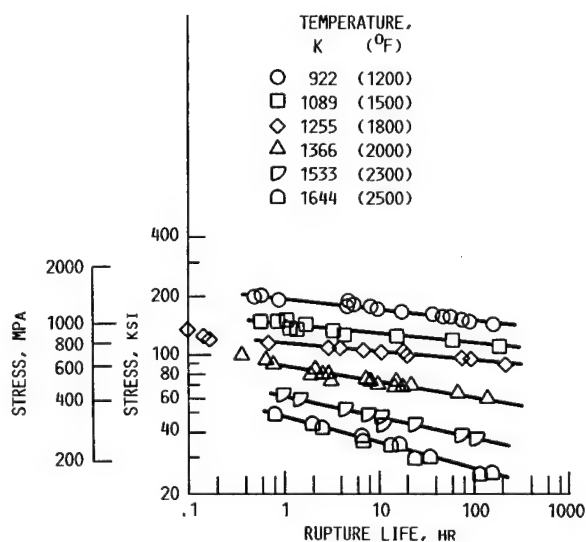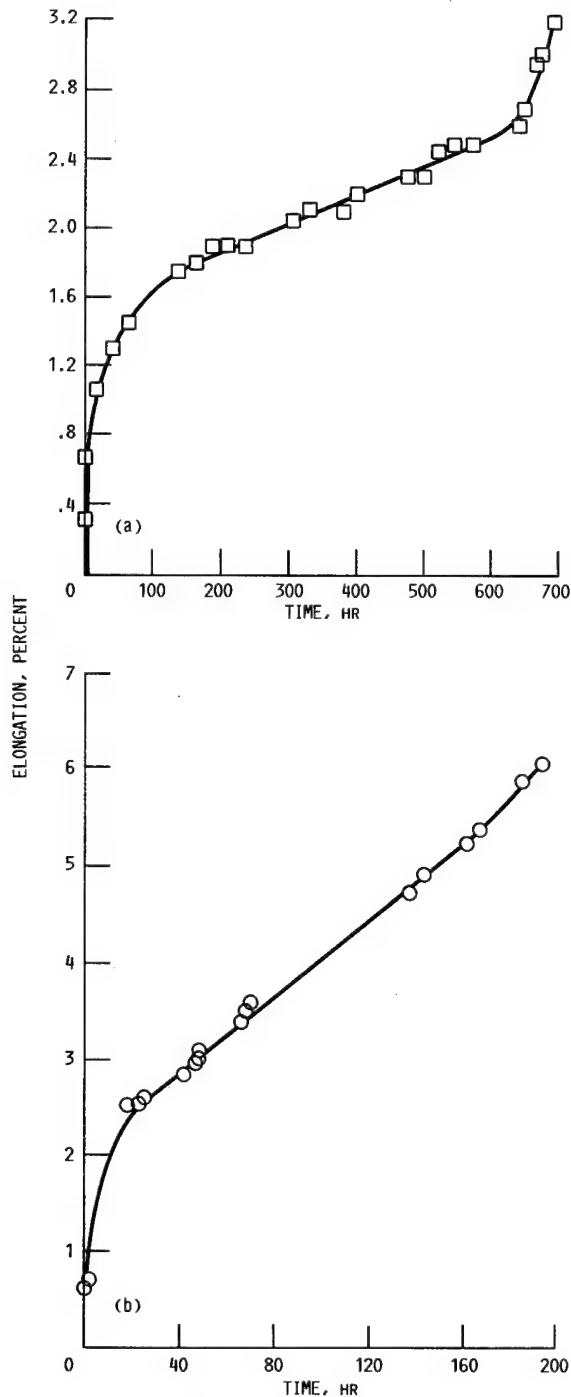

Figure 19.—Effect of stress on rupture life for as-drawn 0.127-mm-(5-mil-) diameter tungsten wire at various temperatures (ref. 15).

9

(a) Tested at 922 K (1200 °F).
(b) Tested at 1089 K (1500 °F).

Figure 20.—Typical creep curves of tungsten fiber reinforced copper matrix composites (ref. 16).

(a) Stress distribution.
(b) Creep curves.

Figure 21.—Schematic of creep curves and stress-distribution curves showing seven stages of creep behavior in tungsten fiber reinforced copper matrix composites (ref. 16).

first-stage creep. As the creep rate decreases, there is a continuing rebalancing of stresses between the fiber and the matrix. If the two components enter into second-stage steady-state creep at different times, then the stronger component, the fiber, forces the weaker matrix to adopt its deformation behavior after a short transition period. This change in the normal behavior of the components gives rise to a quasi-first-stage creep governed by the creep characteristics of the fiber.

Eventually a balance is reached between work-hardening and recovery, and a constant creep rate is attained. With the attainment of second-stage creep, with its constant creep rate, there is an additional rebalancing of stresses between the components. This stress equilibrium is maintained for a fairly high fraction of test life.

(a) Stress, 655 MPa (95 000 psi).
(b) Stress, 552 MPa (80 000 psi).
(c) Stress, 517 MPa (75 000 psi).
(d) Stress, 483 MPa (70 000 psi).
(e) Stress, 448 MPa (65 000 psi).
(f) Stress, 414 MPa (60 000 psi).
(g) Stress, 345 MPa (50 000 psi).
(h) Stress, 276 MPa (40 000 psi).
(i) Stress, 207 MPa (30 000 psi).
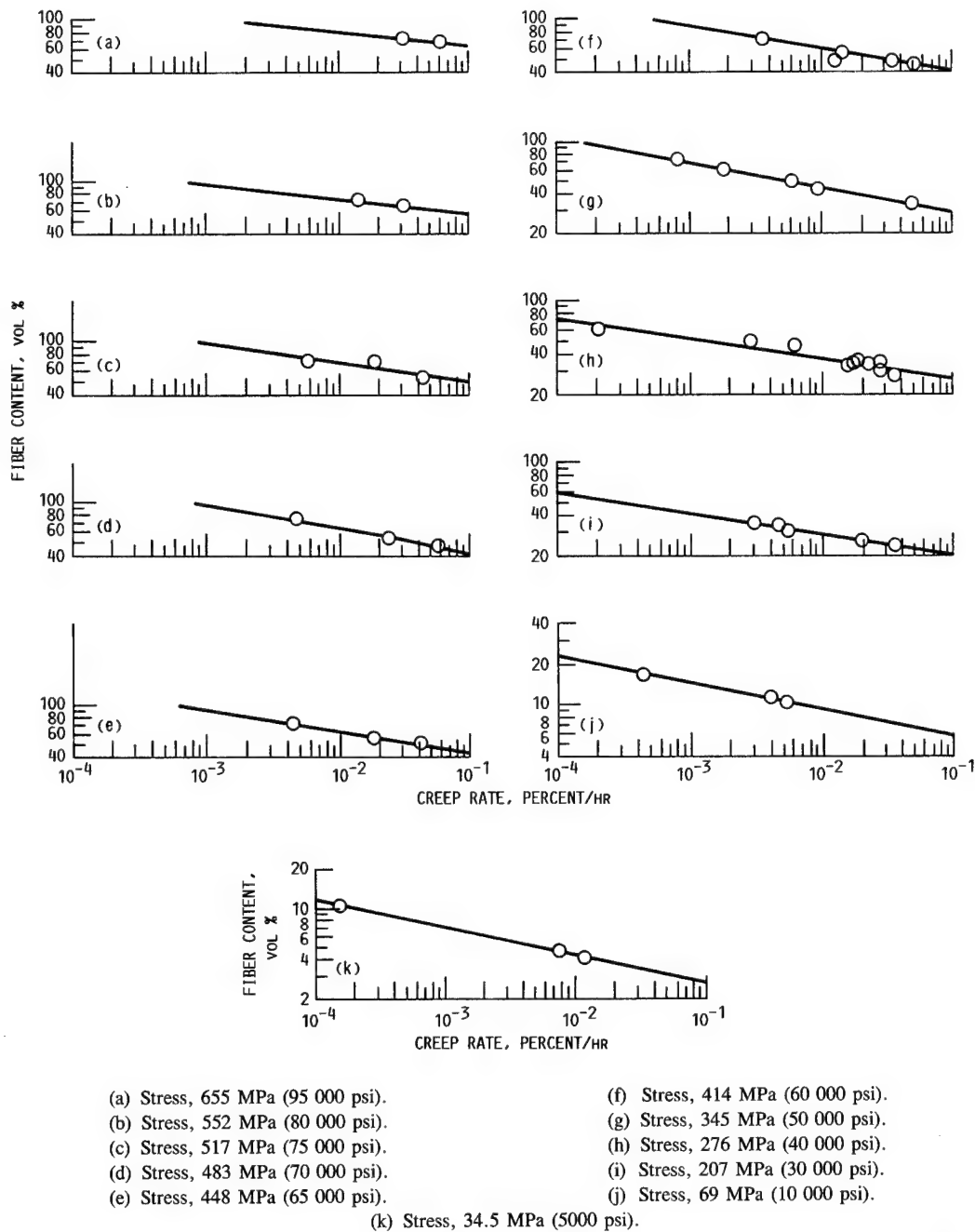(j) Stress, 69 MPa (10 000 psi).
(k) Stress, 34.5 MPa (5000 psi).

Figure 22.—Fiber content as function of creep rate at various stresses for tungsten fiber reinforced copper matrix composites tested at 1089 K (1500 °F) (ref. 16).

After a constant second-stage creep rate is established, the stress on the composite which causes a given creep rate may be calculated from a log-stress/log-creep-rate curve. If the equilibrium of forces is considered, the stress distribution on the fiber and matrix can be predicted by

$$\sigma_{c_{\dot{\epsilon}}} = \sigma_{f_{\dot{\epsilon}}} V_f + \sigma_{m_{\dot{\epsilon}}} V_m \qquad (9)$$

where $\sigma_{c_{\dot{\epsilon}}}$ is the stress on the composite to give a creep rate of $\dot{\epsilon}$, and $\sigma_{f_{\dot{\epsilon}}}$ and $\sigma_{m_{\dot{\epsilon}}}$ are the stresses on the fiber and on the

matrix to give a creep rate of $\dot{\epsilon}$. Since it is difficult to experimentally measure creep rates for fibers, this equation allows fiber creep rates, (at various stresses and temperatures), to be calculated when the creep rate of the composite is measured and the stress to cause that creep rate is known for the matrix material.

The creep rates of W/Cu composites were measured experimentally and a log-fiber-content/log-creep-rate relation was plotted for a series of composite stresses. An example of these plots is shown in figure 22. The fiber contents required

11

for a given creep rate were taken from these curves and were plotted for each composite stress in figure 23 to give a rule-of-mixtures relation of composite stress to fiber content for a series of creep rates. Extrapolation of these data in the low fiber content region showed that the stresses for a given creep rate are in good agreement with the creep rates for unreinforced copper at these temperatures.
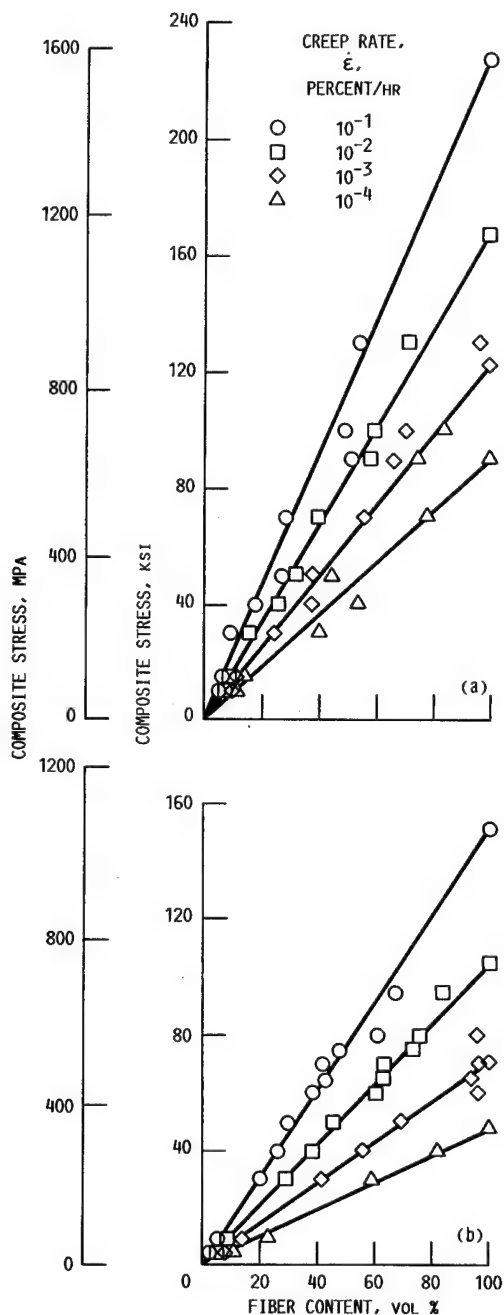
(a) Test temperature, 922 K (1200 °F).
(b) Test temperature, 1089 K (1500 °F).

Figure 23.—Stress for a given creep rate as function of fiber content for tungsten fiber reinforced copper matrix composites (ref. 16).

After a period of second-stage creep, most materials pass into third-stage creep. Again, the onset of third-stage creep may occur at different times for the fiber and the matrix. Materials such as copper show a considerable amount of third-stage creep prior to failure. From the data for W/Cu composites in this investigation, it appears that, for the same rupture time, the tungsten wire remained in second-stage creep for a much longer time than the copper matrix. Since the fiber and the matrix are bonded together in the composite, the stronger, rate-controlling component—the fiber—forces the more easily deformed matrix to remain in second-stage creep. This process gives rise to a quasi-second-stage creep behavior in the composite. This behavior reduces the stress on the matrix to a value that enables it to remain in second-stage creep. The lowering of the stress on the matrix is compensated by an increase in the stress on the fiber. Quasi-second-stage creep would be expected to continue until the rate-controlling fiber enters third-stage creep, at which time a new stress distribution would be set up between the fiber and the matrix (fig. 21).
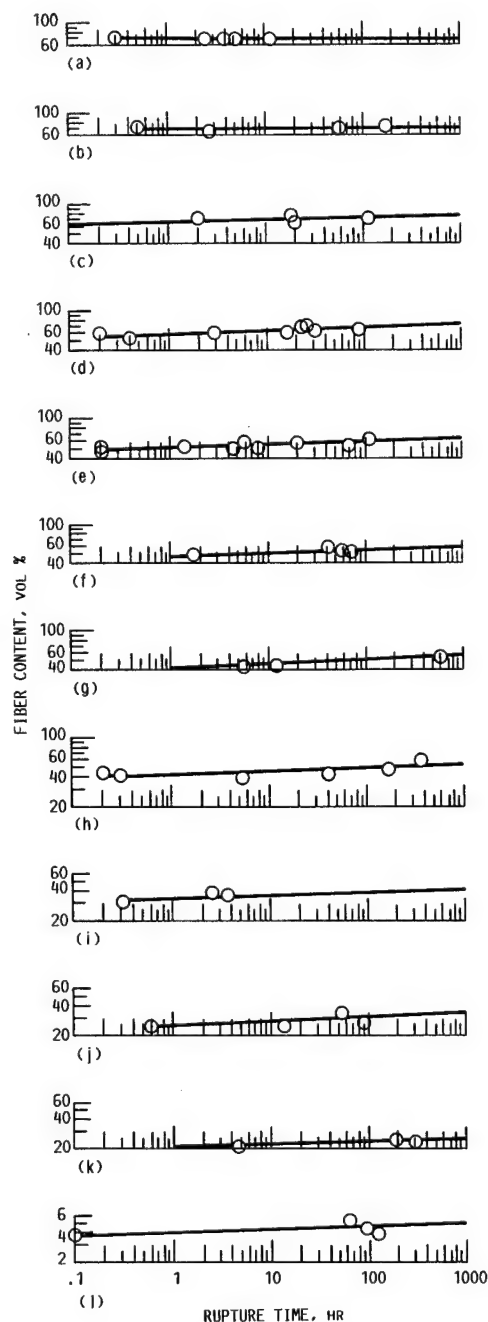
Third-stage creep continues until the fibers start to fail and the initiation of composite fracture begins. The individual fibers in a composite have a scatter band of rupture times at a given stress. The fibers within the composite would be expected to have a scatter band similar to that of fibers tested externally. As the first fibers start to fail at random locations, the remaining fibers in the composite must support a stress slightly higher than that originally encountered when all the fibers were intact. With successive fiber fracture, the actual stress on the remaining fibers continues to increase. Eventually, the stress exceeds the strength of the remaining fibers, and the composite fractures. The actual time to rupture would depend on the number of fibers present and on the rupture-time scatter band of the fibers.

Results of stress-rupture tests indicated that the rupture time of a composite may be predicted by a rule-of-mixtures type relation similar to that used to predict composite creep rates. For a given composite stress, the log of the rupture time is a function of the log of the fiber content (fig. 24). This data was used to determine the fiber contents required for given rupture times for a number of composite stresses as shown in figure 25. This plot shows that a linear rule-of-mixtures relation exists between the composite stress and the fiber content for a given rupture time. The stress to cause rupture of a composite at a given time can be predicted from the properties of the fiber and matrix by

$$\sigma_{c_t} = \sigma_{f_t} V_f + \sigma_{m_t} V_m \qquad (10)$$

where the stress on a composite to cause rupture in time t can be calculated when the stress-rupture properties of the fiber and matrix are known. Handbook values or experimental data can be used directly in equation (10) to predict the properties of composites.
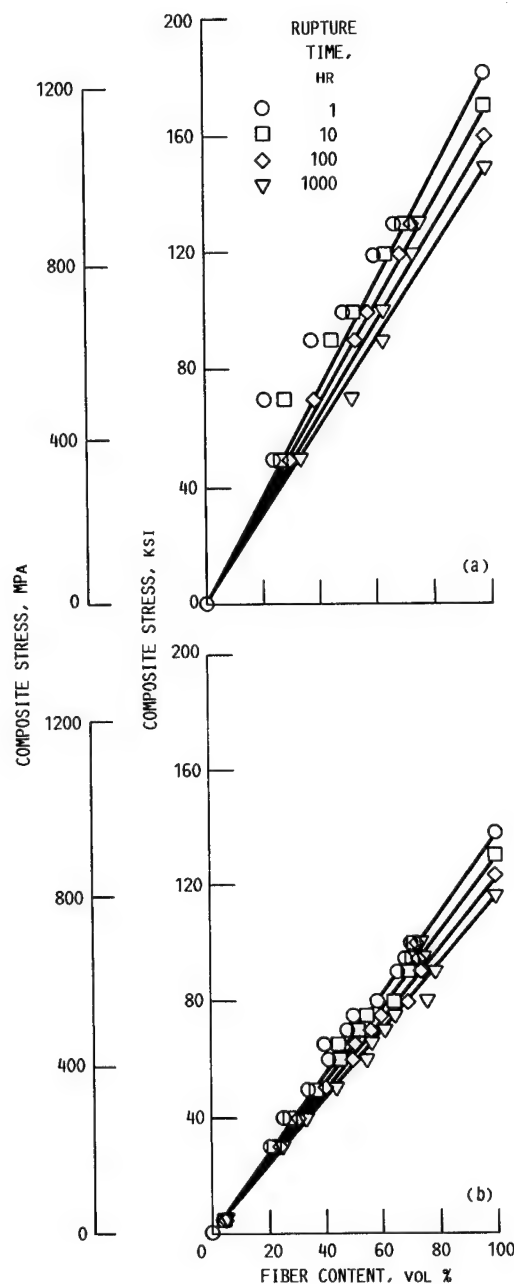
The fracture behavior observed from the stress-rupture tests of W/Cu composites indicated that the stress redistributions postulated during quasi-second-stage and third-stage creep were valid. Unreinforced copper had a brittle stress-rupture failure with a very small reduction in area and with a great deal of intercrystalline cracking at the fracture edge. This brittle behavior is typical of materials tested at a very high fraction of their melting points.

(a) Stress, 690 MPa (100 000 psi).
(b) Stress, 655 MPa (95 000 psi).
(c) Stress, 621 MPa (90 000 psi).
(d) Stress, 552 MPa (80 000 psi).
(e) Stress, 517 MPa (75 000 psi).
(f) Stress, 483 MPa (70 000 psi).
(g) Stress, 448 MPa (65 000 psi).
(h) Stress, 414 MPa (60 000 psi).
(i) Stress, 345 MPa (50 000 psi).
(j) Stress, 276 MPa (40 000 psi).
(k) Stress, 207 MPa (30 000 psi).
(l) Stress, 34.5 MPa (5000 psi).

Figure 24.—Fiber content as function of rupture time at various stresses for tungsten fiber reinforced copper matrix composites tested at 1089 K (1500 °F) (ref. 16).

(a) Test temperature, 922 K (1200 °F).
(b) Test temperature, 1089 K (1500 °F).

Figure 25.—Stress to cause rupture in 1, 10, 100, and 1000 hr as function of fiber content for tungsten fiber reinforced copper matrix composites (ref. 16).

The incorporation of a small amount of reinforcing fibers (about 10 vol %) changed this brittle behavior to a very ductile failure in which the copper almost formed a point at fracture. Since there was no intercrystalline stress-rupture cracking in the matrix, it appears that the matrix of the composite failed in second-stage creep and did not undergo a large amount of third-stage creep as normally found in copper. The majority of strain probably occurred almost instantaneously after the fibers fractured.

Composites with higher fiber contents had a less ductile fracture. Although the fibers had about the same reduction in area as when tested externally (about 80 percent), the composites had an apparent ductility of about 20 percent reduction in area. The fiber/matrix bond had been destroyed at the fracture plane during necking of the fibers, and the fibers continued to neck in their normal behavior until they failed. The copper matrix between the fibers would then start into third-stage creep for a short time until the fibers broke, at which time the entire load would be imposed on the matrix and the remaining matrix would fail instantaneously.

Although the W/Cu composites tested in this study were chosen primarily as a mutually insoluble model system, the results showed that these composites were very strong. In figure 26, the 100-hr rupture strength and the 100-hr rupture-strength/density ratio at 1089 K (1500 °F) of two superalloys commonly used in this temperature range are compared with those of W/Cu composites. The plot shows that at intermediate fiber contents the 100-hr rupture strength of the composites compares favorably with the superalloys. At higher fiber contents (>60 vol %), the properties of the W/Cu composites were superior to those of the superalloys. In spite of the high density of the tungsten wire, the 100-hr rupture-strength/density ratio of the W/Cu composites also compares favorably with that of the superalloys. These results are even more remarkable when considering that the 100-hr rupture strength of unreinforced copper at 1089 K (1500 °F) is 2.6 MPa (0.379 ksi), whereas a 50 vol % W/Cu composite has a 100-hr rupture strength of about 483 MPa (70 ksi).

The stress-rupture and creep results obtained in this W/Cu model system study served as the basis for methods of predicting potential metal matrix composite behavior at high temperatures and demonstrated the feasibility of using tungsten fiber reinforced composites for this type of application. Investigations of other fibers, such as W-$1ThO_2$ and W-$2ThO_2$, W-$3Re$, W-$0.3Hf$-$0.04C$, and W-$4Re$-$0.4Hf$-$0.02C$ alloys, have demonstrated much better high-temperature tensile and creep properties than for unalloyed 218CS-tungsten wire (ref. 17). These fibers were prime candidates for the development of tungsten fiber reinforced superalloy matrix composites (ref. 2).

In addition to the stress-rupture and creep tests conducted on continuous-fiber W/Cu composites, tests were also conducted to determine the effect of critical aspect ratio on the stress-rupture life of discontinuous-fiber composites (ref. 18).

(a) 100-hr rupture-stress fiber content.

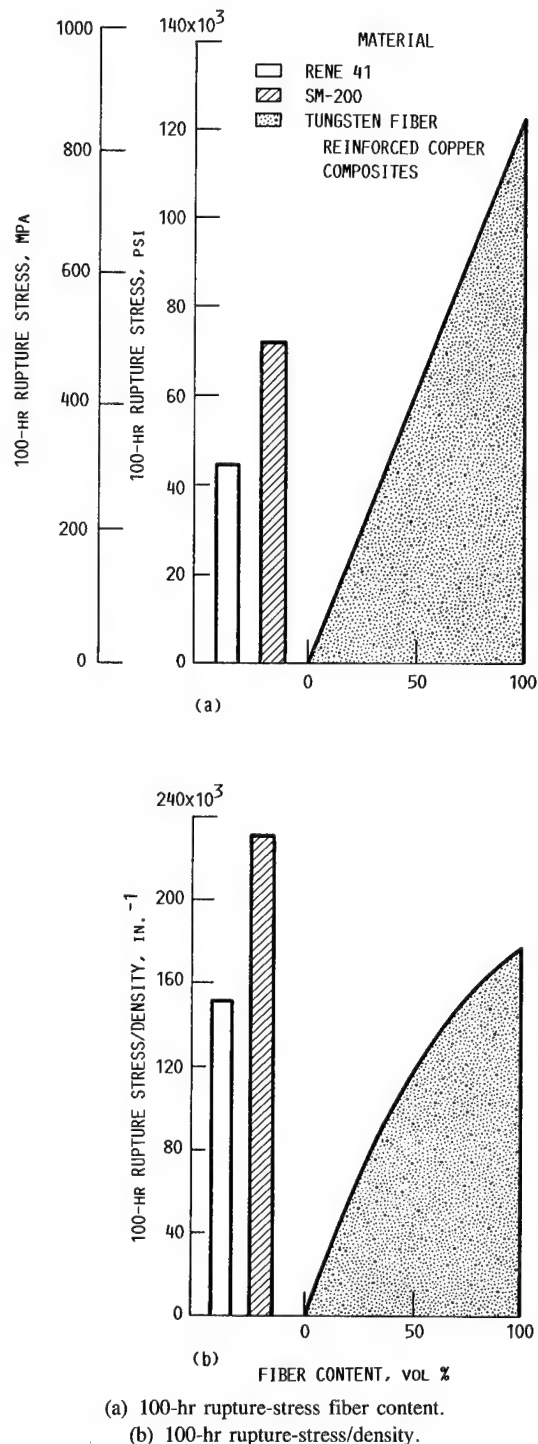(b) 100-hr rupture-stress/density.

Figure 26—Comparison of 100-hr rupture-stress and 100-hr rupture-stress/density ratio for tungsten fiber reinforced copper matrix composites and superalloys at 1089 K (1500 °F) (ref. 16).

Button-head pullout specimens with 0.254-mm-(10-mil-) diameter tungsten wire infiltrated with copper were tested at 922 and 1089 K (1200 and 1500 °F) for nominal shear pullout stress-rupture times of 1, 10, and 100 hr. These tests used the same type of pullout specimen mentioned earlier and reported in reference 11. A summary of the results is shown in figure 27. The observed critical aspect ratios were greater than in short-time tensile tests but were within the same order of magnitude at the test temperatures used. Failure times were controlled by the shear properties of the copper matrix at fiber embedment lengths less than the critical aspect ratio, and by the tensile properties of the tungsten fiber at lengths greater than the critical aspect ratio.

These results indicate that the critical aspect ratio at 1089 K (1500 °F) has only to be lengthened from about 15 for short-time tensile tests to about 30 for a 1000-hr life in stress-rupture service. The most significant result reported in reference 18 deals with the joining of metal matrix composites for high-temperature service. Extrapolation of the results to a higher strength 0.38-mm-(15-mil-) diameter W-2ThO$_2$ wire in a nickel alloy matrix indicates that a fiber length of only 1.14 cm (0.45 in.) would be required to achieve the critical length for 1000-hr stress-rupture life at 1366 K (2000 °F). At the critical length, the reinforcement would only be 50 percent efficient, but increasing the fiber length to 11.5 cm (4.53 in.) would increase the efficiency to 95 percent. Therefore composite panels could be joined with a simple scarf joint with an overlap of only 5.75 cm (2.27 in.) for a 95-percent-efficient joint for 1000-hr stress-rupture life at 1366 K (2000 °F). The same efficiency could be obtained for short-time tensile applications at 1366 K (2000 °F) with an overlap of 2.28 cm (0.90 in.).
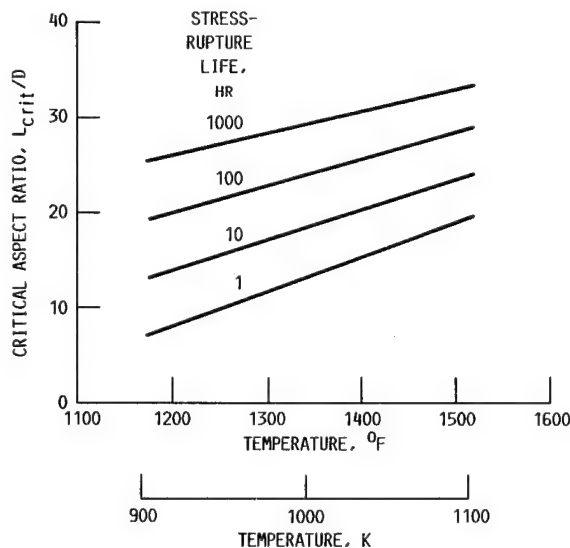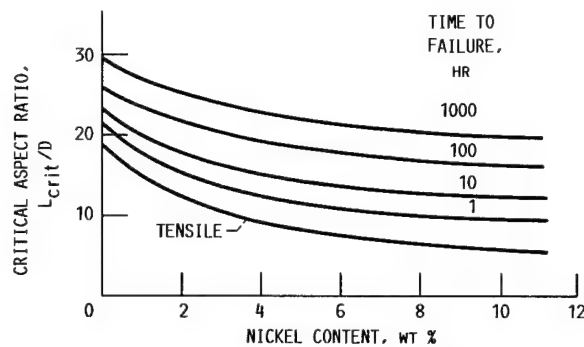

Figure 28.—Critical aspect ratio in tension and stress-rupture for tungsten-wire/copper-nickel alloy pullout specimens tested at 1089 K (1500 °F) (ref. 19).

Shear stress-rupture pullout tests were also used to investigate the effect of alloy matrix composition on the critical aspect ratio (ref. 19). Tungsten fiber pullout specimens were fabricated using copper alloys containing up to 10 wt % nickel. Nickel is soluble in tungsten, and nickel additions to copper matrices caused recrystallization of the tungsten fiber and reduction in strength and ductility of the composites. However, alloy additions of nickel would also increase the shear strength of the copper matrix, and reaction with the fiber should tend to increase the strength of the fiber/matrix interface. The results of these tests indicated that nickel additions to the copper matrix reduced the critical aspect ratio both in short-time tensile tests and in long-time shear stress-rupture tests (fig. 28). This reduction in critical aspect ratio was caused by two factors: the weakening of the tensile and stress-rupture strength of the fiber and the increase in the shear strength of the matrix and the fiber/matrix interface.

Impact Behavior of Tungsten Fiber Reinforced Copper Matrix Composites

Materials for advanced gas turbine blades and vanes must have high stress-rupture strength, oxidation resistance, and impact damage resistance. As part of the W/Cu composite model system program, pendulum impact tests (using a modified Bell Telephone Laboratory type miniature Izod testing machine (ref. 20)) were conducted from room temperature to 810 K (1000 °F) on notched and unnotched miniature Izod specimens. Results of room-temperature impact tests are shown in figure 29. Unnotched specimens with less than 39 vol % fiber content bent in a ductile manner and were forced out of the testing machine without breaking. When the fiber content was higher than 39 vol %, the W/Cu composites broke on impact, with the impact strength decreasing with increasing fiber content. In tests at 420 and 810 K (300 and 1000 °F),

Figure 27.—Calculated critical aspect ratios of tungsten-wire/copper pullout specimens in stress rupture (ref. 18).

all specimens bent in a ductile manner while absorbing an impact value in excess of 12.88 J (114 in.-lb) prior to being forced out of the testing machine. Notched miniature Izod specimens were also tested and fractured at an impact strength below that of the unnotched specimens.

Subsequent studies were conducted to determine the effect of changing fiber or matrix toughness on the impact strength of W/Cu composites (ref. 21). A set of specimens were fabricated at an infiltration temperature of 1700 K (2600 °F), which caused partial recrystallization of the tungsten fibers. Partial recrystallization of the wires reduced the tensile strength and ductility of the composites. This thermal treatment reduced the impact strength of the composites at room temperature. However the impact strength approached that of the unrecrystallized-fiber composites at 810 K (1000 °F).

The impact behavior of the W/Cu composite is controlled by the relative toughness and ductility of the fiber and the matrix and by the volume fraction of each component. Because of their mutual insolubility, there is no fiber/matrix reaction, and the bond between the fiber and the matrix is primarily mechanical in nature. The impact strength of the composites is primarily a measure of energy absorbed during elastic-plastic deformation of the fibers and the matrix. The ductile-to-brittle transition temperature (DBTT) of as-drawn tungsten wires is around room temperature. W/Cu composites fabricated at 1478 K (2200 °F) also had a DBTT around room temperature, whereas the partially recrystallized fiber W/Cu composites had a DBTT somewhat above room temperature. The unalloyed copper matrix is ductile at all testing temperatures, whereas the tungsten fibers are ductile above their DBTT. Both types of W/Cu composites were above their DBTT at elevated temperatures and showed ductile impact behavior (ref. 21).

Impact specimens with Cu-7Ni or Cu-10Ni alloy matrices showed a more brittle behavior (ref. 21). Unreinforced copper-
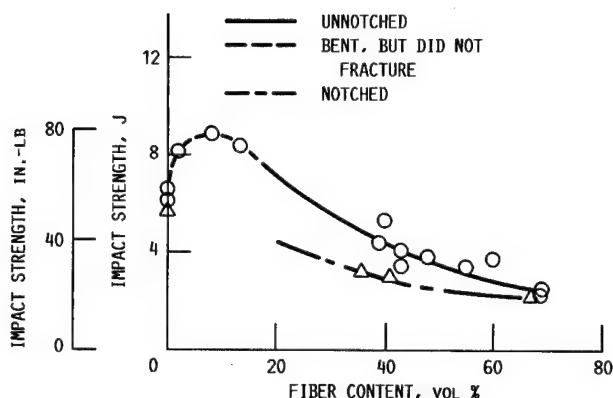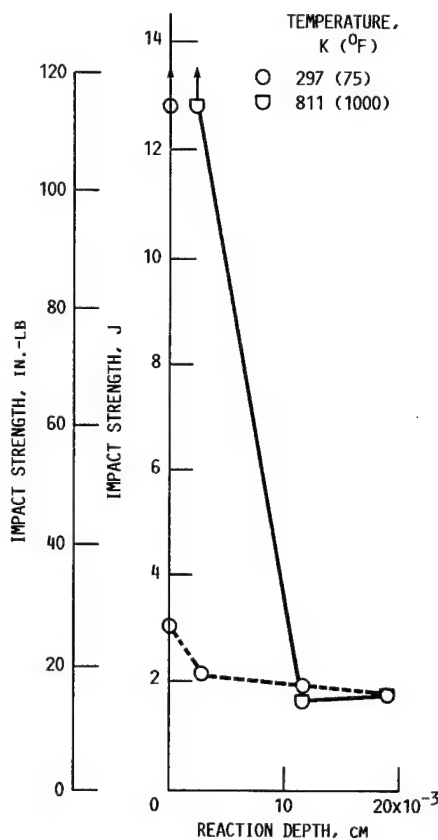

Figure 30.—Effect of reaction depth on impact strength of unnotched tungsten fiber reinforced copper-nickel alloy matrix composites; fiber content, approximately 55 vol % (data from ref. 21).

nickel alloys had lower impact strengths than unalloyed copper at room temperature. Nickel alloy additions to copper also cause recrystallization in the fiber and reduce the strength and ductility of the composite. The amount of property degradation is a function of the extent of the diffusion-triggered recrystallization in the fiber (fig. 18). The impact test results showed similar results and indicated that the greater the depth of penetration of the diffusion-triggered penetration-recrystallization zone, the lower the impact strength and ductility of the copper-nickel alloy matrix composites (fig. 30). At small reaction depths, the composites were brittle at room temperature but were ductile at elevated temperatures. With larger reaction depths, the Cu-Ni matrix composites exhibited brittle behavior throughout their entire testing range up to 811 K (1000 °F) and did not exhibit a transition to ductile behavior.

Electrical Conductivity of Tungsten Fiber Reinforced Copper Matrix Composites

Copper and tungsten are two of the best electrical conductors available. As part of the evaluation and analysis of the W/Cu
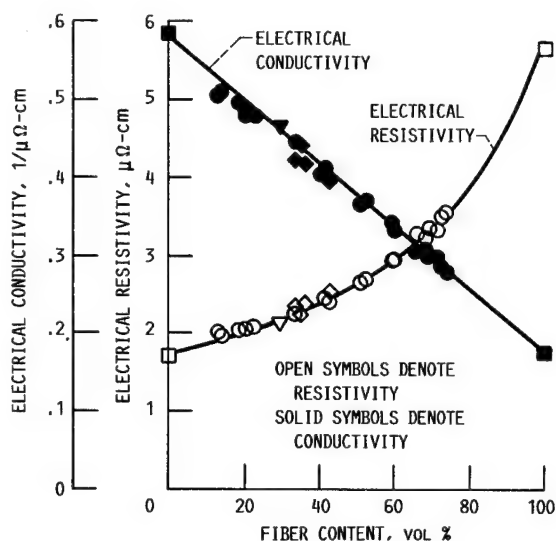

Figure 29.—Effect of fiber content on room-temperature impact strength of tungsten fiber reinforced copper matrix composites (ref. 20).

Figure 31.—Electrical resistivity and conductivity of tungsten fiber reinforced copper matrix composites (ref. 22).
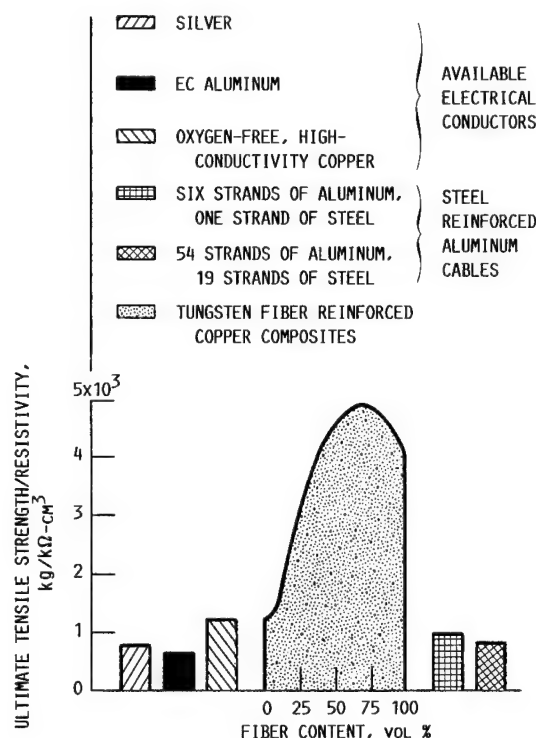

Figure 32.—Comparison of ultimate tensile strength/resistivity ratios for tungsten fiber reinforced copper matrix composites with those for other electrical conductors (ref. 22).

composites program, composites covering a wide range of fiber contents were fabricated and tested to determine the effect of fiber content on room-temperature electrical resistivity and conductivity (ref. 22).

Results of electrical resisitivity and its reciprocal, conductivity, are plotted in figure 31 as a function of fiber content. These results showed that the electrical resistivity was a hyperbolic function of fiber content and that the electrical conductivity was a linear rule-of-mixtures function of fiber content. The electrical conductivity of the composites can be expressed as

$$K_c = K_f V_f + K_m V_m \qquad (11)$$

where K is the electrical conductivity and V is the volume fraction of the fiber or matrix.

Because of the high strength and relatively high electrical conductivity of W/Cu composites, they have potential as practical, high-strength electrical conductors. By combining a W/Cu composite electrical conductor as a structural member, significant potential weight savings could be gained in spacecraft applications. Since high-strength electrical conductors require materials that are a compromise between strength and conductivity, ratios of ultimate tensile strength to resistivity were compared for various materials. The values for W/Cu composites are plotted over a range of fiber contents in figure 32 and are compared to current conductors and high-strength electrical cables. The strength-to-resistivity ratio for W/Cu composites increased rapidly above a fiber content of about 10 vol %, reached a maximum at about 70 vol %, and then fell off to that of the tungsten wire. The ratio of strength

to resistivity for W/Cu composites in the 50 to 75 vol % fiber range was about three to seven times that of the other conductors.

For applications where density is also important, the materials were also compared on the basis of ultimate tensile strength/density-to-resistivity ratio in figure 33. The ratio increased with increasing fiber content to reach a maximum at about 50 vol % and then dropped to the value of tungsten wire. The plot shows that W/Cu composites, with a fiber content of 50 to 60 vol %, are about 10 to 15 percent better than the best high-strength electrical cable available, about 30 percent better than aluminum, and more than twice as good as copper.

These plots show that W/Cu composites have good potential as high-strength, high-electrical-conductivity materials. A fiber content of 55 to 60 vol % would probably be the best compromise between electrical conductivity, strength, and strength/density. A further potential advantage is that with their very high tensile and creep strengths shown at elevated temperatures, W/Cu composites could also be used at much higher temperatures than current electrical conductors. This would allow the composites to carry increased current amperages without structural damage since conductor overheating would be a far less severe problem than with standard conductors.
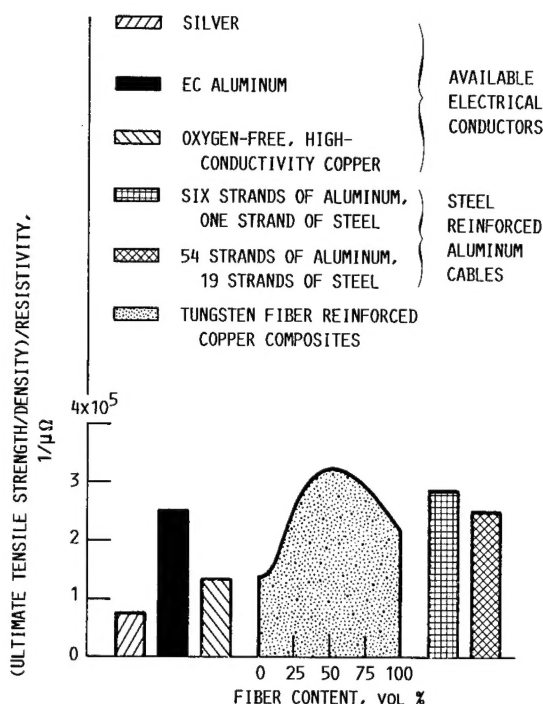
Figure 33.—Comparison of ultimate tensile strength/density-to-resistivity ratios for tungsten fiber reinforced copper composites with those for other electrical conductors (ref. 22).

Thermal Conductivity of Tungsten Fiber Reinforced Copper Matrix Composites

Because of the good high-temperature strength and electrical conductivity shown by W/Cu composites, they also could have a good potential as high-strength, elevated-temperature thermal conductivity materials, since thermal conductivity is usually proportional to electrical conductivity. Efforts are currently underway to apply W/Cu composites to rocket thrust chamber liners to take advantage of the high-temperature strength and thermal conductivity properties of W/Cu composites.

Advanced rocket engines, such as the space shuttle main engine, must be capable of repeated use. As a consequence, the combustion chamber walls must undergo numerous thermal cycles with significant thermal strain. Currently these high-pressure thrust chambers are life-limited because of plastic strain levels encountered in the hot-gas-side wall during each thermal cycle. This high strain level is caused by the large hot-gas-side wall to outer-surface wall temperature difference that exists during the burn portion of the cycle. The large plastic strains from these repeated thermal cycles appear to cause thinning of the cooling passage wall at the centerline until the wall thins to a point where it can no longer sustain the high pressure load and finally fails in fatigue as shown in figure 34. The failed section of the chamber wall is indicated by the arrow in the photograph.

Based on the good high-temperature properties of W/Cu composites, a preliminary fabrication demonstration and testing program was conducted to determine the feasibility of using W/Cu composites as rocket thrust chamber combustion liner materials. Materials for the composites, which were chosen on the basis of strength and thermal conductivity, were a 0.2-mm-(8-mil-) diameter W-3Re (type 3D, General Electric Co.) fiber and a Cu-0.15Zr (Amzirc) matrix (which has about the same thermal conductivity as OFHC copper). Fiber content was selected from design projections of the strength and thermal conductivity of W/Cu composites for a minimum-weight configuration (figs. 35 and 36). The goal was to get a strength improvement over the current liner material, NARloy-Z (Cu-3Ag-0.5Zr) (Rocketdyne Div., Rockwell International Corp.), with a minimal loss in thermal conductivity.

The strength and thermal cycle behavior of W/Cu composites were determined by fabricating and testing W/Cu composite tubes. A 10 vol % fiber content was chosen to meet the strength, conductivity, and weight requirements. The
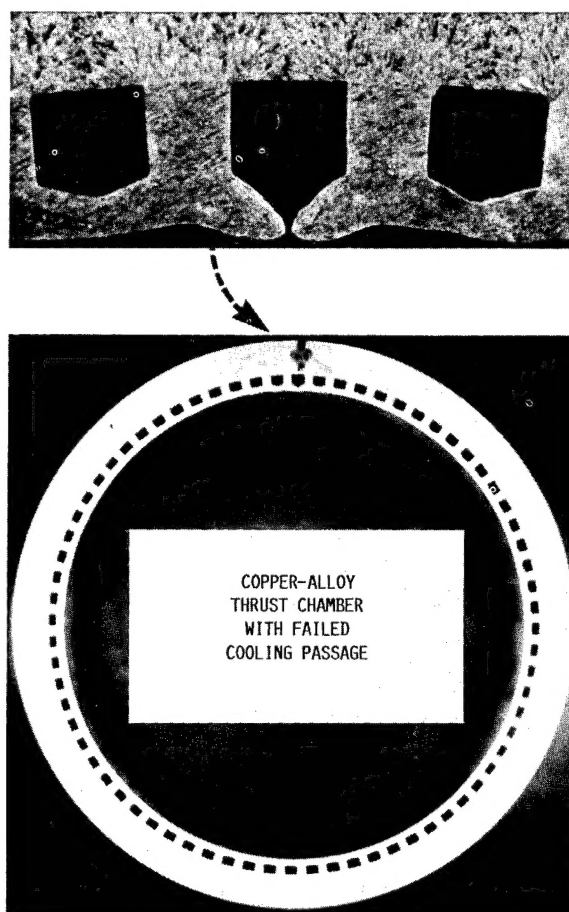

Figure 34.—Rocket thrust chamber with enlargement of fatigue failure in cooling passage wall (ref. 23).

composite tubes were 8.5 times stronger than similar unreinforced copper tubes in internal pressurization tests at 1228 K (1700 °F). In addition, the W/Cu composite tubes were thermal cycled from 339 to 866 K (150 to 1100 °F) and exhibited no thermal distortion after 2000 cycles. Several cylindrical combustion liner test specimens were fabricated for future evaluation in rocket engine test firings (fig. 37). The final phase of the program made a subscale combustion liner fabrication demonstration structure in which a one-third size, hour-glass-shaped composite combustion liner was successfully fabricated (fig. 38).

Figure 37.—Tungsten fiber reinforced copper matrix cylindrical combustion liner test specimen (ref. 23).
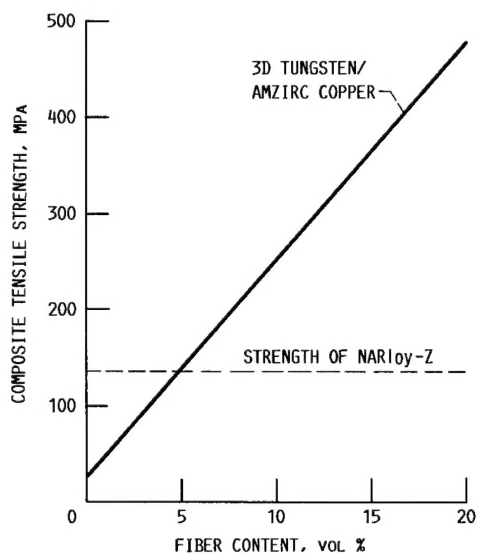

Figure 35.—Effect of fiber content on projected tensile strength of tungsten fiber reinforced copper-alloy matrix composites at 866 K (1100 °F) (ref. 23).
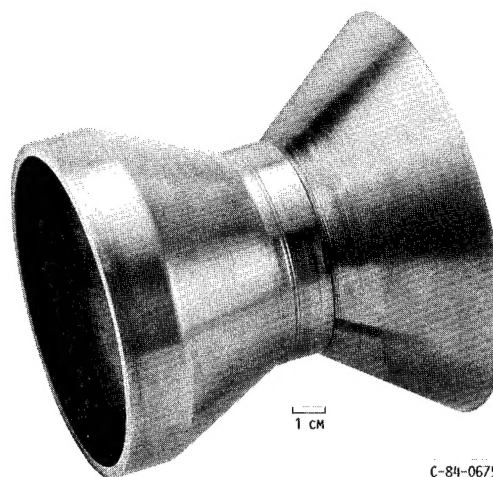
Figure 38.—Subscale tungsten fiber reinforced copper matrix combustion liner demonstrating fabrication feasibility (ref. 23).

Concluding Remarks

NASA Lewis Research Center conducted a series of research programs to evaluate the properties of tungsten fiber reinforced copper matrix composites. The W/Cu composite system was chosen as a model system because of the mutual insolubility of tungsten and copper which allowed the individual properties of the fiber and matrix to be related to the properties of the composites. Most of the composites studied had pure copper matrices, but some copper alloys also were studied to give insight into diffusion-reaction kinetics. In the course of these studies, stress-strain behavior, tensile and creep behavior, and impact and conductivity behavior were analyzed.
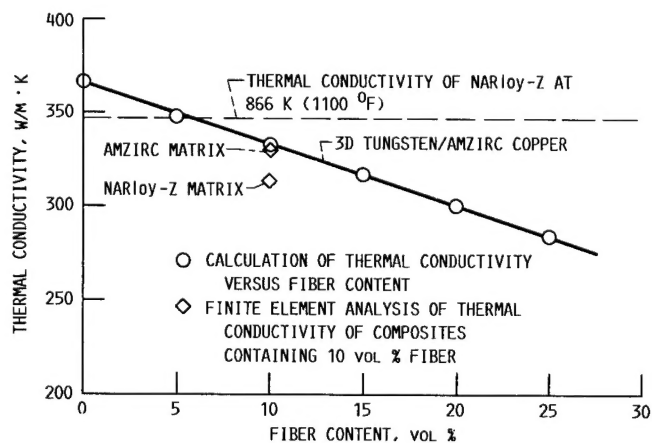

Figure 36.—Effect of fiber content on projected thermal conductivity of tungsten fiber reinforced copper-alloy matrix composites at 866 K (1100 °F) (ref. 23).
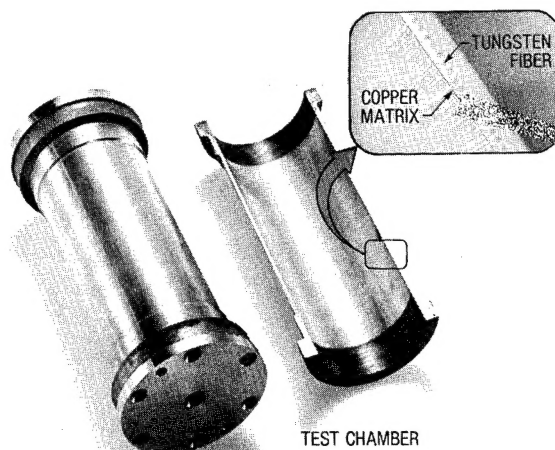
The choice of the W/Cu composite system and the use of liquid infiltration fabrication allowed composites to be made over a wide range of fiber contents. Therefore, a number of specimens could be made and tested so that properties could be analyzed in depth. Because the tungsten fibers and the copper matrix were mutually insoluble, the properties of each component could be evaluated independently. Because the tungsten fibers and the copper matrix form a strong bond at the fiber/matrix interface, the components of the composite always strain equally, with the actual strain being a stress-strain-related balance between the properties of the two components. The rule-of-mixtures predictions were developed by analyzing these stress-strain relations.

At the time of the initial W/Cu studies, metal matrix composites technology was in its infancy. The high-strength W/Cu composites tested in these studies generated a great deal of interest and the rule-of-mixtures analyses first developed in these studies gave the initial impetus for the development of metal matrix composites. Since then, the rule-of-mixtures relations developed in these studies have been universally adopted as the criteria for measuring composite efficiency. Although most of this work was aimed at analyzing W/Cu composites as a model system, the practical uses of their properties were recognized. Thus, these composites are being considered for specialized aerospace high-temperature, high-strength, high-conductivity applications.

Lewis Research Center
National Aeronautics and Space Administration
Cleveland, Ohio, April 6, 1989

References

1. McDanels, D.L.; Serafini, T.T.; and DiCarlo, J.A.,: Polymer, Metal and Ceramic Matrix Composites for Advanced Aircraft Engine Applications. J. Mater. Energy Systems, vol. 8, no. 1, June 1986, pp. 80–91. (Also, NASA TM–87132.)

2. Petrasek, D.W.; and Signorelli, R.A.: Tungsten Fiber Reinforced Superalloys—A Status Review. Fabrication of Composite Materials Source Book, M.M. Schwartz, ed., American Society for Metals, Metals Park, OH, 1985, pp. 14–81. (Also, NASA TM–82590.)

3. McDanels, D.L.; and Signorelli, R.A.: Improvement of High Velocity Ballistic Impact Behavior of Boron/Aluminum Composites. NASA TM–83683, 1984.

4. Jech, R.W.; McDanels, D.L.; and Weeton, J.W.: Fiber Reinforced Metallic Composites. Composite Materials and Composite Structures, Syracuse University Press, Syracuse, NY, 1959, pp. 116–139.

5. McDanels, D.L.; Jech, R.W.; and Weeton, J.W.: Metals Reinforced with Fibers. Met. Prog., vol. 78, no. 6, Dec. 1960, pp. 118–121.

6. McDanels, D.L.; Jech, R.W.; and Weeton, J.W.: Stress-Strain Behavior of Tungsten-Fiber-Reinforced Copper Composites. NASA TN D–1881, 1963.

7. McDanels, D.L.; Jech, R.W.; and Weeton, J.W.: Analysis of Stress-Strain Behavior of Tungsten-Fiber-Reinforced Copper Composites. Trans. Met. Soc. AIME, vol. 233, no. 4, Apr. 1965, pp. 636–642.

8. Petrasek, D.W.: Elevated-Temperature Tensile Properties of Alloyed Tungsten Fiber Composites. Trans. Met. Soc. AIME, vol. 236, no. 6, June 1966, pp. 887–896. (Also, NASA TN D–3073.)

9. Petrasek, D.W.; Signorelli, R.A.; and Weeton, J.W.: Metallurgical and Geometrical Factors Affecting Elevated-Temperature Tensile Properties of Discontinuous Tungsten-Fiber-Reinforced Composites. Fiber Strengthened Metallic Composites, ASTM STP–427, American Society for Testing and Materials, 1967, pp. 149–175. (Also, NASA TN D–3886.)

10. Kelly, A.; and Tyson, W.R.: Fibre Strengthened Materials. High-Strength Materials, V.F. Zackay, ed., John Wiley & Sons, NY, 1965, pp. 578–602.

11. Jech, R.W.; and Signorelli, R.A.: The Effect of Interfiber Distance and Temperature on the Critical Aspect Ratio in Composites. NASA TM X–52347, 1967. (Also, NASA TN D–4548.)

12. Petrasek, D.W.; and Weeton, J.W.: Alloying Effect on Tensile Properties and Micro-Structure of Tungsten-Fiber-Reinforced Composites. NASA TN D–1568, 1963.

13. Petrasek, D.W.; and Weeton, J.W.: Effects of Alloying on Room-Temperature Properties of Tunsten-Fiber-Reinforced Copper-Alloy Composites. Trans. Met. Soc. AIME, vol. 230, no. 5, Aug. 1964, pp. 977–990.

14. Jech, R.W.; Springborn, R.H.; and McDanels, D.L.: Apparatus for Stress-Rupture Testing of Filaments in a Controlled Atmosphere. Rev. Sci. Instrum., vol. 35, no. 3, Mar. 1964, pp. 314–315.

15. McDanels, D.L.; and Signorelli, R.A.: Stress-Rupture Properties of Tungsten Wire From 1200 to 2500 °F. Met. Eng. Q., vol. 6, no. 3, Aug. 1966, pp. 51–58. (Also, NASA TN D–3467.)

16. McDanels, D.L.; Signorelli, R.A.; and Weeton, J.W.: Analysis of Stress-Rupture and Creep Properties of Tungsten Fiber Reinforced Cooper Composites. Fiber Strengthened Metallic Composites, ASTM STP–427, American Society for Testing and Materials, Philadelphia, PA, 1967, pp. 124–148. (Also, NASA TN D–4173.)

17. Petrasek, D.W.: High-Temperature Strength of Refractory-Metal Wires and Consideration for Composite Applications. NASA TN D–6881, 1972.

18. Jech, R.W.: Influence of Fiber Aspect Ratio on the Stress-Rupture Life of Discontinuous fiber Composites. NASA TN D–5735, 1970.

19. Jech, R.W.: Critical Aspect Ratio for Tungsten Fibers in Copper-Nickel Matrix Composites. NASA TM X–3311, 1975.

20. Winsa, E.A.; and Petrasek, D.W.: Pendulum Impact Resistance of Tungsten-Fiber Metal-Matrix Composites. Composite Materials: Testing and Design, ASTM STP–497, American Society for Testing and Materials, Philadelphia, PA, 1972, pp. 350–362. (Also, NASA TM X–67810.)

21. Winsa, E.A.; and Petrasek, D.W.: Factors Affecting Miniature Izod Impact Strength of Tungsten-Fiber-Metal Matrix Composites. NASA TN D–7393, 1973.

22. McDanels, D.L.: Electrical Resistivity and Conductivity of Tungsten Fiber Reinforced Copper Composites. Trans. ASM, vol. 59, Dec. 1966, pp. 994–997. (Also, NASA TN D–3590.)

23. Westfall, L.J.; and Petrasek, D.W.: Fabrication and Preliminary Evaluation of Tungsten Fiber Reinforced Copper Composite Combustion Chamber Liners. NASA TM–100845, 1988.

NASA
National Aeronautics and
Space Administration

Report Documentation Page

1. Report No. NASA TP-2924	2. Government Accession No.	3. Recipient's Catalog No.
4. Title and Subtitle Tungsten Fiber Reinforced Copper Matrix Composites—A Review		5. Report Date September 1989
		6. Performing Organization Code
7. Author(s) David L. McDanels		8. Performing Organization Report No. E-4318
		10. Work Unit No. 586-01-11
9. Performing Organization Name and Address National Aeronautics and Space Administration Lewis Research Center Cleveland, Ohio 44135-3191		11. Contract or Grant No.
		13. Type of Report and Period Covered Technical Paper
12. Sponsoring Agency Name and Address National Aeronautics and Space Administration Washington, D.C. 20546-0001		14. Sponsoring Agency Code

15. Supplementary Notes

16. Abstract

Tungsten fiber reinforced copper matrix (W/Cu) composites have served as an ideal model system with which to analyze the properties of metal matrix composites. A series of research programs were conducted to investigate the stress-strain behavior of W/Cu composites; the effect of fiber content on the strength, modulus, and conductivity of W/Cu composites; and the effect of alloying elements on the behavior of tungsten wire and of W/Cu composites. Later programs investigated the stress-rupture, creep, and impact behavior of these composites at elevated temperatures. Analysis of the results of these programs has allowed prediction of the effects of fiber properties, matrix properties, and fiber content on the properties of W/Cu composites. These analyses formed the basis for the rule-of-mixtures prediction of composite properties which has been universally adopted as the criteria for measuring composite efficiency. In addition, the analyses allowed extrapolation of potential properties of other metal matrix composites and were used to select candidate fibers and matrices for development of tungsten fiber reinforced superalloy composite materials for high-temperature aircraft and rocket engine turbine applications. This report summarizes the W/Cu composite efforts conducted at NASA Lewis Research Center, describes some of the results obtained, and provides an update on more recent work using W/Cu composites as high-strength, high-thermal-conductivity composite materials for high heat flux, elevated-temperature applications.

17. Key Words (Suggested by Author(s)) Metal matrix composites; Copper; Tungsten; Tensile strength; Stress-strain behavior; Stress-rupture strength; Creep rate; Electrical conductivity; Thermal conductivity	18. Distribution Statement Unclassified—Unlimited Subject Category 24

19. Security Classif. (of this report) Unclassified	20. Security Classif. (of this page) Unclassified	21. No of pages 24	22. Price* A03